Two-stage mode finder for waveguides with a 2D cross-section

P. Bienstman (peter.bienstman@ugent.be)
Ghent University / IMEC, Sint-Pietersnieuwstraat 41, 9000 Gent, Belgium

Abstract. We present a fast and efficient method to find the vectorial eigenmodes of waveguides with an arbitrary 2D cross-section. The method can deal with both material losses and radiation losses (through Perfectly Matched Layer boundary conditions). In the first stage of the method, a coarse estimate of the propagation constants is found using a plane-wave method. In the second stage, these estimates are refined using a mode-matching method.

Keywords: waveguide, modelling, PML

1. Introduction

Finding propagation constants and mode profiles of the vectorial eigenmodes of waveguides with an arbitrary two-dimensional cross-section is an important problem in integrated optics. Here, we present an efficient method which combines the virtues of plane-wave expansion methods and mode-matching methods. In a first stage, a plane-wave method is used to construct a single eigenvalue problem which provides an estimate of the eigenmodes of the structure. These estimates are subsequently refined in the second stage using a technique based on vectorial eigenmode expansion. We opt for a vectorial eigenmode expansion technique because evidence suggests that it can deal more accurately with discontinuities and singularities which inevitably occur in the field profiles of these eigenmodes (Sudbø, 1992).

The mode-matching method we present here is related to the one described in (Sudbø, 1993a) and (Sudbø, 1993b), but uses a slightly different set of basis functions (complex exponentials rather than geometric functions) and a different approach to derive the dispersion relation. We also generalise it to include Perfectly Matched Layer (PML) boundary conditions. Additionally, the two-stage technique to efficiently locate the eigenmodes in the complex plane has to our knowledge not been described before.

The rest of this paper is organised as follows. In Section 2 we will describe the basis functions used in the mode-matching model. These will be used in Section 3 to perform a generalised mode matching and to calculate scattering matrices. Section 4 builds on this to derive the transcendental dispersion relation whose solutions give the eigenmodes

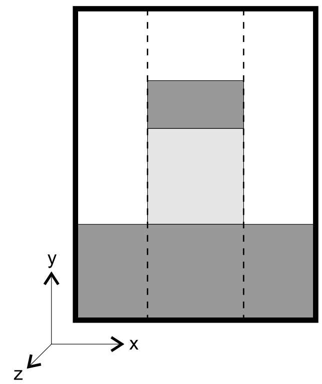

Figure 1. Waveguide with a 2D cross-section

of the waveguide. In Section 5 we will outline how to efficiently find the complex solutions of this function by using a two-stage method. A non-trivial example of a lossy photonic wire in Silicon-on-Insulator (SOI) with be given in Section 6.

2. Rotated basis functions

Suppose we want to calculate the eigenmodes of the waveguide shown in Fig. 2.

The waveguide is enclosed in metal walls which can be coated with a Perfectly Matched Layer (PML). The philosophy behind eigenmode expansion is to divide the structure into a number of slices where the index profile is invariant in one direction. In Fig. 2, this direction is the x-direction, and three slices can be identified. Subsequently, the field in each slice is expanded in a set of basis functions, and later we will apply continuity equations to calculate the transition between two slices.

To derive this set of basis functions in each slice, we consider each slice as a 1D waveguide (infinite in the x-direction) and calculate its TE and TM eigenmodes (propagating in the x-direction) (Sztefka and Nolting, 1993; Bienstman and Baets, 2001). These have the following form for TE:

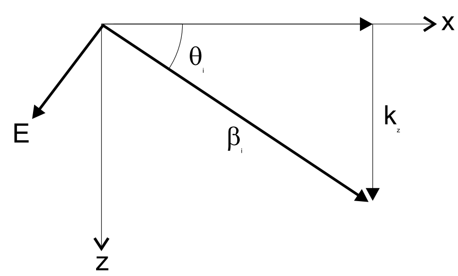

Figure 2. Rotating the mode profile over an angle θ_i

$$\left\{\begin{array}{lcl} E_{x,i,TE} & = & 0 \\ E_{y,i,TE} & = & 0 \\ E_{z,i,TE} & = & E_{z,i,TE,0}\left(y\right)\cdot\exp\left(-j\beta_i x\right) \\ H_{x,i,TE} & = & H_{x,i,TE,0}\left(y\right)\cdot\exp\left(-j\beta_i x\right) \\ H_{y,i,TE} & = & H_{y,i,TE,0}\left(y\right)\cdot\exp\left(-j\beta_i x\right) \\ H_{z,i,TE} & = & 0 \end{array}\right. \tag{1}$$

For TM, we get:

$$\left\{\begin{array}{lcl} E_{x,i,TM} & = & E_{x,i,TM,0}\left(y\right)\cdot\exp\left(-j\beta_i x\right) \\ E_{y,i,TM} & = & E_{y,i,TM,0}\left(y\right)\cdot\exp\left(-j\beta_i x\right) \\ E_{z,i,TM} & = & 0 \\ H_{x,i,TM} & = & 0 \\ H_{y,i,TM} & = & 0 \\ H_{z,i,TM} & = & H_{z,i,TM,0}\left(y\right)\cdot\exp\left(-j\beta_i x\right) \end{array}\right. \tag{2}$$

In these equations, i is the index of the mode. The k-vector of these slice eigenmodes lies entirely in the (x, y)-plane (no z-component), which makes them unsuited to expand the field of an eigenmode of the entire cross-section. Such a cross-section eigenmode has a k-vector component along z which is constant across the cross-section. Therefore, to expand its field, we will rotate all the slice eigenmodes around the y-axis until their k-vector has a z-component equal to an arbitrary but fixed value k_z (see Fig. 2 for TE). (We will later discuss how to determine the values of k_z that give rise to eigenmodes of the cross-section.) For each slice mode i, this means rotating the field profile with an angle θ_i given by

$$\sin\theta_i = \frac{k_z}{\beta_i} \tag{3}$$

This results in the following TE basis functions:

$$\begin{cases} E_{x,i,TE} &= -\sin\theta_i \cdot E_{z,i,TE,0}\left(y\right) \cdot \exp\left(-j\beta_i x\right) \\ E_{y,i,TE} &= 0 \\ E_{z,i,TE} &= \cos\theta_i \cdot E_{z,i,TE,0}\left(y\right) \cdot \exp\left(-j\beta_i x\right) \\ H_{x,i,TE} &= \cos\theta_i \cdot H_{x,i,TE,0}\left(y\right) \cdot \exp\left(-j\beta_i x\right) \\ H_{y,i,TE} &= H_{y,i,TE,0}\left(y\right) \cdot \exp\left(-j\beta_i x\right) \\ H_{z,i,TE} &= \sin\theta_i \cdot H_{x,i,TE,0}\left(y\right) \cdot \exp\left(-j\beta_i x\right) \end{cases} \tag{4}$$

For TM, this becomes:

$$\begin{cases} E_{x,i,TM} &= \cos\theta_i \cdot E_{x,i,TM,0}\left(y\right) \cdot \exp\left(-j\beta_i x\right) \\ E_{y,i,TM} &= E_{y,i,TM,0}\left(y\right) \cdot \exp\left(-j\beta_i x\right) \\ E_{z,i,TM} &= \sin\theta_i \cdot E_{x,i,TM,0}\left(y\right) \cdot \exp\left(-j\beta_i x\right) \\ H_{x,i,TM} &= -\sin\theta_i \cdot H_{z,i,TM,0}\left(y\right) \cdot \exp\left(-j\beta_i x\right) \\ H_{y,i,TM} &= 0 \\ H_{z,i,TM} &= \cos\theta_i \cdot H_{z,i,TM,0}\left(y\right) \cdot \exp\left(-j\beta_i x\right) \end{cases} \tag{5}$$

3. Generalised mode matching

The next problem is to calculate the reflection and transmission matrices of an interface between two different slices (named e.g. I and II), once again for a given fixed value of k_z. Since TE and TM components will be coupled at the interface, we need to include both kinds of modes in our basis set. We now develop a generalisation of the well-known mode-matching technique (see e.g. (Sztefka and Nolting, 1993)). It starts off by exciting the interface with only mode p from medium I and by imposing the continuity of the tangential components of the total field:

$$\mathbf{E}^{I}_{p,t} + \sum_j R_{j,p}\mathbf{E}^{I}_{j,t} = \sum_j T_{j,p}\mathbf{E}^{II}_{j,t} \tag{6}$$

$$\mathbf{H}^{I}_{p,t} - \sum_j R_{j,p}\mathbf{H}^{I}_{j,t} = \sum_j T_{j,p}\mathbf{H}^{II}_{j,t} \tag{7}$$

To calculate the unknown expansion coefficients $R_{j,p}$ and $T_{j,p}$ we take the right cross product of Eq. 6 with $\mathbf{H}^{II}_{i,t}$ and the left cross product of Eq. 7 with $\mathbf{E}^{I}_{i,t}$. Here, i is an arbitrary index. After integrating over the cross-section, we get:

$$\left\langle \mathbf{E}^{I}_{p}, \mathbf{H}^{II}_{i} \right\rangle + \sum_j R_{j,p}\left\langle \mathbf{E}^{I}_{j}, \mathbf{H}^{II}_{i} \right\rangle = \sum_j T_{j,p}\left\langle \mathbf{E}^{II}_{j}, \mathbf{H}^{II}_{i} \right\rangle \tag{8}$$

$$\left\langle \mathbf{E}_i^I, \mathbf{H}_p^I \right\rangle - \sum_j R_{j,p} \left\langle \mathbf{E}_i^I, \mathbf{H}_j^I \right\rangle = \sum_j T_{j,p} \left\langle \mathbf{E}_i^I, \mathbf{H}_j^{II} \right\rangle \tag{9}$$

where the scalar product is defined as the following overlap integral:

$$\langle \mathbf{E}_m, \mathbf{H}_n \rangle \equiv \int \int_s (\mathbf{E}_m \times \mathbf{H}_n) \cdot \mathbf{u}_x dS \tag{10}$$

If we decide to truncate the series expansion after N modes (which includes both TE and TM modes), we have $2N$ unknowns: N reflection coefficients and N transmission coefficients. Eq. 8 and 9 provide us with exactly $2N$ equations, since we can write them for all i in $1 \to N$.

The traditional mode matching algorithm then proceeds to simplify this system of equations by invoking orthogonality relations between the modes. In this case however, this is not possible because rotated TE modes are not orthogonal to rotated TM modes under the scalar product of Eq. 10.

We can repeat this procedure for every incident mode p in $1 \to N$, which ultimately gives rise to the following system of equations to calculate the $\mathbf{R}$ and $\mathbf{T}$ matrices:

$$\begin{bmatrix} \mathbf{O}_{II,II}^T & -\mathbf{O}_{I,II}^T \\ \mathbf{O}_{I,II} & \mathbf{O}_{I,I} \end{bmatrix} \cdot \begin{bmatrix} \mathbf{T} \\ \mathbf{R} \end{bmatrix} = \begin{bmatrix} -\mathbf{O}_{I,II}^T \\ \mathbf{O}_{I,I} \end{bmatrix} \tag{11}$$

Here, T denotes transposition and the overlap matrices are defined as

$$\mathbf{O}_{A,B}(i,j) \equiv \left\langle \mathbf{E}_i^A, \mathbf{H}_j^B \right\rangle \tag{12}$$

A and B are either I or II. Calculating these matrices from Eq. 4 and Eq. 5 is straightforward and involves overlap integrals of the following form:

$$\begin{aligned}
\langle \mathbf{E}_{i,TE}, \mathbf{H}_{j,TE} \rangle &= -\cos\theta_i \int E_{z,i,TE,0} H_{y,j,TE,0} dy \\
\langle \mathbf{E}_{i,TE}, \mathbf{H}_{j,TM} \rangle &= 0 \\
\langle \mathbf{E}_{i,TM}, \mathbf{H}_{j,TE} \rangle &= \sin\theta_j \int E_{y,i,TM,0} H_{x,j,TE,0} dy - \sin\theta_i \int E_{x,i,TM,0} H_{y,j,TE,0} dy \\
\langle \mathbf{E}_{i,TM}, \mathbf{H}_{j,TM} \rangle &= \cos\theta_j \int E_{y,i,TM,0} H_{z,j,TM,0} dy
\end{aligned}$$

Here, the indices i and j refer to modes either from the same medium or from different media. The 1D integrals over y are independent of k_z and therefore need to be calculated only once.

We also need to calculate the $\mathbf{R}$ and $\mathbf{T}$ matrices for incidence from medium II instead of from medium I. Our choice of multiplying Eq. 6 with $\mathbf{H}_{i,t}^{II}$ rather than with the traditional $\mathbf{H}_{i,t}^{I}$ ensures that the system matrix for this new linear system can be chosen identical to the system matrix in Eq. 11, which saves computation time.

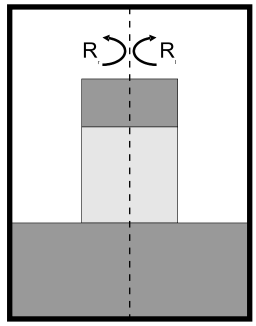

Figure 3. Splitting the waveguide in half

Once we have calculated these reflection and transmission matrices for a single interface, we can proceed in a classical way to calculate these matrices for an entire stack of slices by using the well-known S-matrix scheme (Li, 1996). This method is numerically stable, even in the presence of high-order evanescent modes.

4. Transcendental dispersion relation

We still need to address the problem of determining which values of k_z give rise to actual eigenmodes of the waveguide with the 2D cross-section. For that purpose, we divide the cross-section at an arbitrary position in two halves (Fig. 4). Using the techniques from the previous sections, we can calculate for each value of k_x the reflection matrix $\mathbf{R}_l\,(k_z)$of the left part as seen from the right, and similarly the reflection matrix $\mathbf{R}_r\,(k_z)$of the right part as seen from the left. In case the vector $\mathbf{A}$ corresponds to the expansion of the forward propagating field of an eigenmode at the cut, the following resonance relation will hold:

$$\mathbf{R}_l\,(k_z)\cdot\mathbf{R}_r\,(k_z)\cdot\mathbf{A}=\mathbf{A} \tag{13}$$

In other words, the round trip gain of the eigenmode should be unity. In this way, the problem is reduced to finding the values of k_z for which the matrix $\mathbf{R}_l\cdot\mathbf{R}_r$ has an eigenvalue of unity. The corresponding eigenvector then describes the field profile of that eigenmode.

Finally, we want to explain briefly how PML is incorporated in the method. These boundary conditions are implemented by using complex coordinate stretching (Chew et al., 1997), i.e. by letting the values of the cladding thickness assume complex values. This can be done for the cladding thickness in both the x and y-direction. Care should be taken not to choose this complex thickness excessively large, in order to avoid numerical problems related to completeness issues (Bienstman, 2001).

5. Finding complex solutions of the dispersion relation

In general, the k_z values which satisfy Eq. 13 will be located in the complex plane away from the coordinate axes. This is true when the materials in the waveguide are lossy, but is also true if we want to incorporate PML boundary conditions by giving the claddings a complex thickness (Chew et al., 1997). Finding complex solutions of a transcendental equation like Eq. 13 is a non-trivial problem, especially when a single evaluation of this function takes a non-negligible amount of computation time. It is therefore imperative to develop a method which can find these solutions with a minimum of function evaluations. Also, the method should be robust enough to be able to locate all eigenmodes of the structure (including radiation modes) without skipping any.

There are a number of possible approaches to tackle this problem. A first approach is start by finding the eigenmodes of an identical structure, but where are all loss mechanisms (material and PML absorption) are set to zero. In this way, the modes are located on the coordinate axes, where they are more easily found. We can then gradually change the losses from zero to their final value and track the modes as they move through the complex plane (Bienstman et al., 2001). Although this works fine to find modes in 1D slabs, it is not the best method for modes in waveguides with a 2D cross-section. The reason is that this method still requires a large number of function evaluations, especially when two modes are nearly degenerate. Also, in 2D structures there can exist even in the lossless case modes that are located in the complex plane (for a description of these complex modes, see e.g. (Oliner et al., 1981)).

A second approach to find zeros of a complex function is based on contour integration. There exist a number of variants of this method (Delves and Lynnes, 1967; Anemogiannis et al., 1994), but they basically all involve evaluating a number of complex contour integrals, from which a polynomial is constructed which has the same zeros as the complex function inside the contour. Problem with these methods is that they still require a large number of function evaluations, they need special attention when zeros are located close to the contours, and they mostly do not cope well with branch point singularities.

We therefore propose to use a hybrid method, in which a first stage give us a coarse estimate of the eigenmodes. In a second stage, these estimates are used as initial guesses to a Newton-like method which will converge in a few seconds to the exact solutions using only a handful of iterations.

To construct the initial estimates, we use the plane-wave like method which we described in (Bienstman and Baets, 2003) and which is based on the method proposed in (Omar and Schünenmann, 1987). It involves expanding the eigenmodes into the eigenmodes of a uniform homogeneous waveguide (which are essentially plane waves in the 2D Cartesian case). These uniform waveguide modes are denoted by tildes in the following formula:

$$\begin{cases} \mathbf{E}_{trans} &= \sum A_i \tilde{\mathbf{E}}_{i,trans,TE} + \sum B_i \tilde{\mathbf{E}}_{i,trans,TM} \\ E_z &= \sum C_i \tilde{E}_{i,z,TM} \\ \mathbf{H}_{trans} &= \sum D_i \tilde{\mathbf{H}}_{i,trans,TE} + \sum E_i \tilde{\mathbf{H}}_{i,trans,TM} \\ H_z &= \sum F_i \tilde{H}_{i,z,TE} \end{cases} \tag{14}$$

After some manipulations, we can derive an eigenproblem of the following form:

$$\mathbf{A} \cdot \mathbf{x} = k_z^2 \mathbf{x} \tag{15}$$

Important to note is that k_z appears here in the eigenvalues, and not as a parameter of the matrix like in Eq. 13. So, for N terms retained in the series expansion, we get an estimate for the first N modes, which can subsequently be refined in the second stage.

This method is well-suited to handle degenerate or closely-clustered modes. Their presence is readily detected from the first stage, such that appropriate numerical precautions can be taken in the second stage. These precautions take the form of deflating each refined zero of the cluster before attempting to refine the next zero estimate from the cluster.

Finally, we wish to illustrate why the first stage only yields a coarse estimate. The reason is that the expansion functions in stage 1 are plane waves and therefore continuous across the entire waveguide. Since the mode profile of the eigenmode will be continuous across some interfaces and discontinuous across others, it is clear that such basis functions are ill-suited to expand the eigenmode. In stage 2 however, we use the set of rotated slice modes as basis set. Within each slice, these modes already obey the different interface boundary conditions, and across slices, a different basis set is used. Such a representation is therefore inherently more suited to accurately describe the field. This is shown in Fig. 5, where the E_y component of the (lower left quarter of the) fundamental mode of a square waveguide is plotted, both for a stage 1 expansion with 500 terms, and a stage 2 expansion with 40 terms. The waveguide

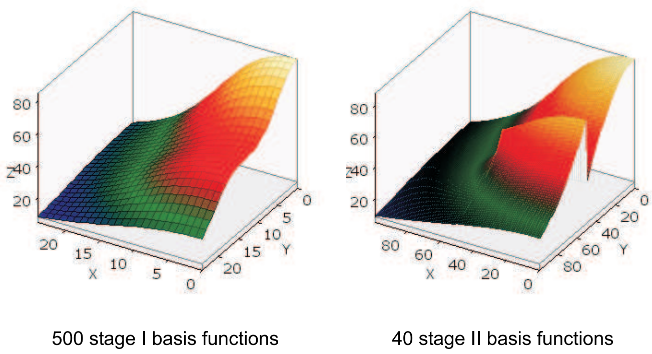

Figure 4. E_y component of fundamental mode of square waveguide (only lower left quarter of waveguide plotted)

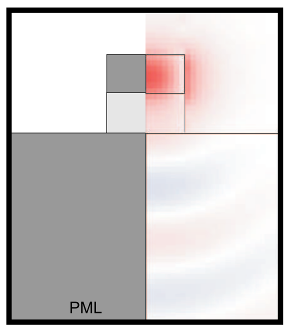

Figure 5. Field profile in a photonic wire

is a square with side of 1λ, with refractive index $n = 1.5$ and embedded in air.

6. Example: SOI photonic wire

As a less trivial example, we calculate the radiation loss at $\lambda = 1.55\,\mu m$ of the fundamental mode of a photonic wire waveguide, consisting of a Si ($n = 3.5$) core with width W and height 220 nm, separated by an oxide ($n = 1.45$) buffer of height D from a Si substrate. For thin buffers, light will leak from the central core to the bottom substrate, as is shown in the plot of E_x in Fig. 6 for $W = .4\,\mu m$ and $D = .2\,\mu m$.

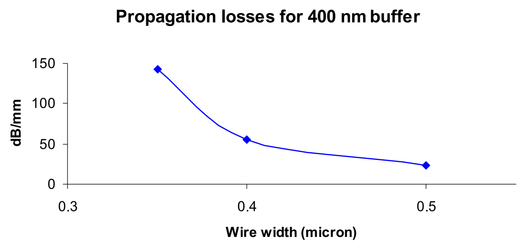

Figure 6. Propagation losses in a photonic wire

From the imaginary part of the propagation constant we can easily derive the propagation loss in dB/mm. In Fig. 6,we plot this propagation loss as a function of W for $D = .4\,\mu m$. As the wire gets narrower, the mode loses confinement, which results in increased propagation losses.

7. Conclusions

We presented an efficient algorithm to calculate the eigenmodes of lossy waveguides with an arbitrary 2D Cartesian cross-section. In a first stage, a coarse estimate of the propagation constants of the first N eigenmodes is constructed using a plane-wave method. These estimates are subsequently refined in a second stage, where the fields are expanded in the rotated eigenmodes of each slice which makes up the waveguide.

Acknowledgments

PB acknowledges the Flemish Fund for Scientific Research (FWO-Vlaanderen) for a postdoctoral fellowship. Parts of this work were performed in the context of the Belgian DWTC project IAP-Photon.

References

Anemogiannis, E., E. N. Glytsis, and T. K. Gaylord: 1994, 'Efficient solution of eigenvalue equations of optical waveguide structures'. *IEEE J. Lightwave Technol.* **12**(12), 2080–2084.

Bienstman, P.: 2001, 'Rigorous and efficient modelling of wavelength scale photonic components'. Ph.D. thesis, Ghent University.

Bienstman, P. and R. Baets: 2001, 'Optical modelling of photonic crystals and VCSELs using eigenmode expansion and perfectly matched layers'. *Opt. Quantum Electron.* **33**, 327–341.

Bienstman, P. and R. Baets: 2003, 'Efficient hybrid method to find eigenmodes of waveguides with a 2D cross-section'. *IEEE J. Quantum Electron.* draft in preparation for submission.

Bienstman, P., H. Derudder, R. Baets, F. Olyslager, and D. De Zutter: 2001, 'Analysis of cylindrical waveguide discontinuities using vectorial eigenmodes and perfectly matched layers'. *IEEE Trans. Microwave Theor. Tech.* **49**(2), 349–354.

Chew, W., J. Jin, and E. Michielssen: 1997, 'Complex coordinate stretching as a generalized absorbing boundary condition'. *Microwave Opt. Technol. Lett.* **15**(6), 363–369.

Delves, L. and J. Lynnes: 1967, 'A numerical method for locating the zeros of an analytic function'. *Math. Comp.* **21**, 543–560.

Li, L.: 1996, 'Formulation and comparison of two recursive matrix algorithms for modeling layered diffraction gratings'. *J. Opt. Soc. Am. A* **13**(5), 1024–1035.

Oliner, A. A., S.-T. Peng, T.-I. Hsu, and A. Sanchez: 1981, 'Guidance and leakage properties of a class of open dielectric waveguides. II. New physical effects'. *IEEE Trans. Microwave Theor. Tech.* **29**(9), 855–869.

Omar, A. S. and K. F. Schünenmann: 1987, 'Complex and backward-wave modes in inhomogeneously and anistropically filled waveguides'. *IEEE Trans. Microwave Theor. Tech.* **35**(3), 268–275.

Sudbø, A.: 1992, 'Why are accurate computations of mode fields in rectangluar dielectric waveguides difficult'. *IEEE J. Lightwave Technol.* **10**(4), 418–419.

Sudbø, A.: 1993a, 'Film mode matching: a versatile numerical method for vector mode field calculations in dielectric waveguides'. *Pure and Applied Optics* **2**, 211–233.

Sudbø, A.: 1993b, 'Numerically stable formulation of the transverse resonance method for vector mode-field calculations in dielectric waveguides'. *IEEE Photon. Technol. Lett.* **5**(3), 342–344.

Sztefka, G. and H. Nolting: 1993, 'Bidirectional eigenmode propagation for large refractive index steps'. *IEEE Photon. Technol. Lett.* **5**(5), 554–557.